# Intelligent Reflecting Surface-Assisted Full-Duplex UAV-Based Mobile Relay Communication

Mengqiu Chai[1], Shengjie Zhao[1(✉)], Yuan Liu[2], Fuqiang Ding[3], Hai Sun[3], and Runqing Jiang[3]

[1] School of Software Engineering, Tongji University, Shanghai 201804, China
{mengqiuchai,shengjiezhao}@tongji.edu.cn
[2] College of Electronic and Information Engineering, Tongji University, Shanghai 201804, China
tjyuanliu@tongji.edu.cn
[3] Shanghai Ideal Information Industry (Group) Co., Ltd, Shanghai, China

**Abstract.** Intelligent reflecting surface (IRS), a promising technology, can intelligently reflect the signals and improve the propagation environment, which makes it further achieve spectrum efficiency for wireless systems in the future. In this paper, we investigate an IRS-assisted full-duplex (FD) unmanned aerial vehicle (UAV) relay system with a source node and a destination node. Due to the obstacles, the source node can not communicate with the UAV-based mobile relay. The IRS on the wall of a building can reflect the signals from the source node to the relay. We aim to maximize the average rate of the system by jointly optimizing the phase shifter of the IRS, the trajectory of the UAV, and the transmit power of the UAV-based relay. On account of the non-convexity of the formulated problem, we propose a novel algorithm based on iteration that divides the problem into three sub-problems by the block coordinate descent and applies the successive convex approximation (SCA) method for obtaining an approximate optimal solution. Simulation results demonstrate the efficiency of our algorithm.

**Keywords:** Intelligent reflecting surface · Full-duplex relay · Phase control · Trajectory optimization

## 1 Introduction

With the incredible increase of the number of wireless devices in the forthcoming fifth-generation networks, the consumption of the network and the spectrum efficiency remain critical issues in the practical application [1]. As a transformative technology, intelligent reflecting surface (IRS) has been proposed to achieve spectrum efficiency with the lower hardware cost [2]. IRS is constituted of an array of IRS passive units that can independently incur a specific phase shift on the

J. Xiong et al. (Eds.): MobiMedia 2021, LNICST 394, pp. 212–223, 2021.
https://doi.org/10.1007/978-3-030-89814-4_16

incident signals [3]. Therefore, IRS can collaboratively improve the propagation environment and ameliorate the quality of the communication with low energy consumption, which makes IRS arouse widespread concern in communication applications [4]. In [5], the authors proposed a practical phase shift model of IRS which can capture the change of phase-dependent amplitude. A tutorial of new challenges when IRS is integrated into wireless networks has been provided in [6]. In [7], an IRS-assisted non-orthogonal multiple access (NOMA) system has been investigated, and a novel algorithm has been proposed to maximize the system throughput over the channel assignment, reflection coefficients, decoding order of NOMA users, power allocation. The asymptotic max-min signal-to-interference-plus-noise ratio (SINR) of an IRS-assisted multiple-input single-output (MISO) system has been studied, and the simulation results verify that IRS outperforms half-duplex relay [8]. The coverage analysis, the probability of signal-to-noise ratio (SNR) gain, and the delay outage rate of IRS-aided communications system have been investigated [9].

Due to the low energy consumption, flexible deployment, on-demand mobile features, unmanned aerial vehicles (UAVs) have been widely used in public and civil domains [10,11]. UAV can not only be connected to the communication network as a new type of mobile equipment but also can mount a flying base station and relay to guarantee the requirement of more complex communication requirement [12,13]. In [14], the authors investigated the energy efficiency in a single UAV-aided relaying system of two static ground nodes and defined an energy-efficiency metric. The outage probability (OP) of an amplify-and-forward (AF) UAV relaying network has been studied, and the mobile device, the UAV's trajectories, and transmit power of UAV can be optimized [15]. The energy harvesting practicality of a UAV-assisted relaying system has been studied in [16]. In [17], the authors have investigated the analytical expressions of outage probability, average bit error rate (BER), and the average capacity of an IRS-assisted half-duplex (HD)-UAV relaying system. However, most of the studies in UAV-based relay systems are in HD mode.

Considering the dense buildings in cities, it is difficult for direct communications in practical conditions, such as the link between two ground nodes with crowded buildings around. So we introduce the UAV and IRS technology into a system where an IRS-assisted FD UAV-based relay in deployed to maximize the average achievable rate. Different from the existing research results [17], we try to maximize the average achievable rate of the system by jointly optimizing the dynamic UAV's trajectory, transmit power of the UAV, and the phase shifter of IRS with the relay working in FD mode. Because multiple variables are coupled together, the problem is non-convex and hard to resolve. We propose an iterative algorithm that can solve the problem efficiently. Simulation results verify the efficiency of our algorithm.

The rest of this paper is organized as follows. Section 2 describes the system model and the formulated problem. In Sect. 3, we propose a joint optimization algorithm with the UAV's trajectory, transmit power of the UAV, and the phase shifter of IRS. Section 4 and Sect. 5 respectively represent the numerical result and conclusions.

## 2 System Model and Problem Formulation

### 2.1 System Model

As shown in Fig. 1, we consider an IRS-assisted FD UAV-based relaying system with one ground source node ($S$), an IRS installed on the building near $S$, a dynamic UAV-based relay station, one ground destination node ($D$). Due to the obstacles, $S$ can not communicate with $D$ and UAV-based relay. Therefore, IRS is introduced into the scenario to assist the communication. The IRS is equipped on the building near $S$ to reflect the signals received from $S$ to the UAV. The UAV-based relay works in the FD mode. To be specific, the UAV can receive and send data at the same time. A three-dimensional (3-D) Cartesian coordinate system is considered for the scenario. Therefore, the horizontal coordinates of $S$, $D$ are denoted as $w_S = [x_S, y_S]^T$, $w_D = [x_D, y_D]^T$ respectively. Besides, the UAV flies from the initial point $w_0$ to the final point $w_f$ at a fixed height $H_U$. For tractability, we divide the UAV's flight time $T$ into $M$ time slots, i.e., $T = M\tau$, where $\tau$ denotes the slot length. The coordinate changes between two time slots can be regarded as constant. Therefore, the UAV's horizontal coordinates changing with time can be given as $w_U[m] = [x_U[m], y_U[m]]^T$, $m \in \mathcal{M} = 1, 2, ..., M$. Accordingly, the flying constraints of the UAV can be given as

$$w_U[1] = w_0, \tag{1a}$$

$$||w_U[m] - w_U[m-1]|| \leq D_{\max}, m = 2, \cdots M \tag{1b}$$

$$w_U[M] = w_f, \tag{1c}$$

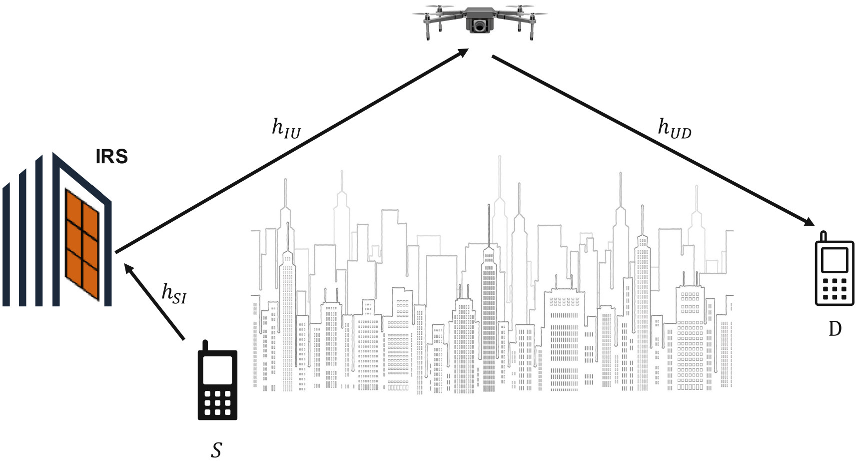

**Fig. 1.** An IRS-assisted DF UAV-based relaying system

where $D_{\max} = V_{\max}\tau$ denotes the maximum distance that the UAV can move at the maximum speed $V_{\max}$ in one time slot.

Moreover, $S$, $D$, and the UAV are all equipped with a single omni-directional antenna. The IRS is equipped with a uniform linear array (ULA) of $N$ elements. A diagonal matrix $\Theta[m] = diag\{e^{j\theta_1[m]}, e^{j\theta_2[m]}, \ldots, e^{j\theta_N[m]}\}$, $\theta_n[m] \in [0, 2\pi)$, $n = 1, 2, \ldots, N$, represents the phase shifter matrix of the IRS in the $m$th time slot. The coordinate and the height of the first element at the IRS are denoted as $w_I = [x_I, y_I]^T$ and $H_I$. We suppose the first element can be regarded as the reference point of the IRS. Therefore, we use $w_I = [x_I, y_I]^T$ and $H_I$ to denote the coordinate and height of the IRS.

## 2.2 Transmission Process

With the obstacles around, the UAV-based relay can not receive the signals from $S$ directly, while the UAV can only receive the signals from $S$ through IRS reflectively. We assume that all channel links are line-of-sight (LoS) channels, and the Doppler effect owing to the movement of UAV can be compensated [18]. The channel coefficient between $S$ and the IRS, $\boldsymbol{h}_{SI} \in \mathcal{C}^{N\times 1}$, can be given as

$$\boldsymbol{h}_{SI} = \sqrt{\gamma d_{SI}^{-2}}[1, e^{-j\frac{2\pi}{\lambda_0}d_0\phi_{SI}}, \ldots, e^{-j\frac{2\pi}{\lambda_0}(N-1)d_0\phi_{SI}}]^T, \tag{2}$$

where $\gamma$ denotes the channel gain at the reference distance $d_{ref} = 1\text{m}$, $d_{SI} = \sqrt{||\boldsymbol{w}_I - \boldsymbol{w}_S||^2 + H_I^2}$ is the distance between $S$ and IRS, $\lambda_0$ is the carrier wavelength, $d_0$ is the antenna separation, $\phi_{SI} = \frac{x_I - x_S}{d_{SI}}$ denotes the cosine of the angle of arrival (AoA) of the signal from $S$ to the IRS.

Similarly, the channel coefficient of the link between IRS and UAV, $\boldsymbol{h}_{IU} \in \mathcal{C}^{N\times 1}$, in the $m$th time slot can be given as

$$\boldsymbol{h}_{IU}[m] = \sqrt{\gamma d_{IU}^{-2}[m]}[1, e^{-j\frac{2\pi}{\lambda_0}d_0\phi_{IU}[m]}, \ldots, e^{-j\frac{2\pi}{\lambda_0}(N-1)d_0\phi_{IU}[m]}]^T, \tag{3}$$

where $d_{IU}[m] = \sqrt{||\boldsymbol{w}_U[m] - \boldsymbol{w}_I||^2 + (H_U - H_I)^2}$ denotes the distance between IRS and UAV, $\phi_{IU}[m] = \frac{x_U[m] - x_I}{d_{IU}[m]}$ is the cosine of the angle of departure (AoD) of the signal from IRS and UAV in the $m$th time slot. It is assumed that a large enough data buffer is equipped on the UAV, which can guarantee the data storage requirement for the decode-and-forward (DF) relay. Therefore, the achievable rate from IRS to UAV can be given as

$$R_S[m] = \log_2\left(1 + \frac{P_S\gamma^2|f[m]|^2}{d_{IU}^2[m]d_{SI}^2\left(\frac{P[m]}{\beta} + \sigma^2\right)}\right), \tag{4}$$

where $f[m] = \sum_{n=1}^{N} e^{j\theta_n[m] + j\frac{2\pi}{\lambda_0}(n-1)d_0(\phi_{IU}[m] - \phi_{SI})}$, $P_S$ denotes the transmit power of $S$, $0 \le \frac{1}{\beta} \le 1$ denotes the self-interference coefficient of FD UAV-based relay, $\sigma$ denotes the additive white Gaussian noise (AWGN) power. Accordingly, in the $m$th time slot, the transmission rate from DF UAV-based relay to $D$ can be given as

$$R_D[m] = \log_2\left(1 + \frac{P[m]\gamma}{d_{UD}^2[m]\sigma^2}\right), \tag{5}$$

where $d_{UD}[m] = \sqrt{||\boldsymbol{w}_U[m] - \boldsymbol{w}_D||^2 + H_U^2}$, $P[m]$ denotes the transmit power of UAV. The average transmission rate of the system $R$ is provided as follow

$$R = \frac{1}{M}\sum_{m=1}^{M} \min\{R_S[m], R_D[m]\}. \tag{6}$$

Due to the limitation of transmit power at UAV, the related power constraints of UAV can be given as

$$\frac{1}{M}\sum_{m=1}^{M} P[m] \leq \bar{P}, \tag{7a}$$

$$0 \leq P[m] \leq P_{\max}, m \in M, \tag{7b}$$

where $\bar{P}$ denotes the average transmit power and $P_{\max}$ denotes the peak transmit power of the UAV.

### 2.3 Problem Formulation

The goal of this paper is to maximize the average rate under the UAV's trajectory constraints (1) and the transmit power constraints (7) with respect to (w.r.t) the variables of UAV's trajectories $\boldsymbol{W}$, the transmit power of the UAV $\boldsymbol{P}$, and the phase shifter of the IRS $\boldsymbol{\Phi}$. Accordingly, the optimal problem can be given as

$$(\mathbf{P}0): \max_{\boldsymbol{W},\boldsymbol{P},\boldsymbol{\Phi}} \ R \tag{8a}$$

$$\text{s.t.} \quad (1), (7). \tag{8b}$$

($\mathbf{P}0$) is not a convex problem and hard to solve. Therefore, we propose a novel algorithm based on iteration to solve ($\mathbf{P}0$) in the next section.

## 3 Proposed Algorithm

In this section, we propose an efficient algorithm to solve ($\mathbf{P}0$). We divide ($\mathbf{P}0$) into three sub-problems and use the block coordinate descent (BCD) method to solve one sub-problem at a time. For tractability, we introduce a variable $\xi$, and ($\mathbf{P}0$) can be transformed as

$$(\mathbf{P}1): \max_{\boldsymbol{W},\boldsymbol{P},\boldsymbol{\Phi}} \ \xi \tag{9a}$$

$$\text{s.t.} \quad (1), (7), \tag{9b}$$

$$\frac{1}{M}\sum_{m=1}^{M} \min\{R_S[m], R_D[m]\} \geq \xi. \tag{9c}$$

### 3.1 Optimization of Phase Shifter

First, we optimize the phase shifter $\boldsymbol{\Phi}$ of IRS with given UAV's trajectories $\boldsymbol{W}$ and transmit power $\boldsymbol{P}$. The maximum value of $f[m]$ is $N$. Therefore, the optimal phase shifter of each elements in the $m$th time slot is

$$\theta_n^{\text{op}}[m] = \frac{2\pi}{\lambda_0}(n-1)d_0(\phi_{SI} - \phi_{IU}[m]). \tag{10}$$

Taking (10) into $R_S[m]$, $R_S[m]$ can be rewritten as

$$R_S^{\text{op}}[m] = \log_2\left(1 + \frac{P_S\gamma^2N^2}{d_{IU}^2[m]d_{SI}^2(\frac{P[m]}{\beta} + \sigma^2)}\right). \tag{11}$$

### 3.2 Optimization of Trajectory

With the optimal phase shifter $\boldsymbol{\Phi}$ and specific transmit power $\boldsymbol{P}$, the sub-problem that optimizes the trajectories of the UAV $\boldsymbol{W}$ is studied in this section. Let $\eta_S[m] = \frac{P_S\gamma^2N^2}{d_{SI}^2(\frac{P[m]}{\beta}+\sigma^2)}$, $\eta_D[m] = \frac{P[m]\gamma}{\sigma^2}$. First, with the variables $\eta_S[m]$ and $\eta_D[m]$, we can respectively rewrite $R_S[m]$ and $R_D[m]$ as

$$G_S[m] = \log_2\left(1 + \frac{\eta_S[m]}{||\boldsymbol{w}_U[m] - \boldsymbol{w}_I||^2 + (H_U - H_I)^2}\right), \tag{12}$$

$$G_D[m] = \log_2\left(1 + \frac{\eta_D[m]}{||\boldsymbol{w}_U[m] - \boldsymbol{w}_D||^2 + H_U^2}\right). \tag{13}$$

Therefore, ($\mathbf{P}1$) can be reformulated as ($\mathbf{P}2$) can be transformed into

$$(\mathbf{P}2): \max_{\boldsymbol{W}} \ \xi \tag{14a}$$

$$\text{s.t.} \ \ (1), \tag{14b}$$

$$\frac{1}{M}\sum_{m=1}^{M} \min\{G_S[m], G_D[m]\} \geq \xi. \tag{14c}$$

Because the constraint (14c) is non-convex w.r.t $\boldsymbol{W}$, which makes ($\mathbf{P}2$) hard to solve. It is worth noting that $G_S[m]$ is convex w.r.t the term $||\boldsymbol{w}_U[m] - \boldsymbol{w}_I||^2$. Consequently, by applying the first-order Taylor expansion of $G_S[m]$ at $||\boldsymbol{w}_U[m] - \boldsymbol{w}_I||^2$ in the $k$th iteration, the lower-bound of $G_S[m]$, denoted as $G_S^{\text{lb}}[m]$, can be written as

$$\begin{aligned} G_S[m] \geq& \log_2\left(1 + \frac{\eta_S[m]}{||\boldsymbol{w}_U^k[m] - \boldsymbol{w}_I||^2 + (H_U - H_I)^2}\right) \\ &- \zeta_S^k[m]\left(||\boldsymbol{w}_U[m] - \boldsymbol{w}_I||^2 - ||\boldsymbol{w}_U^k[m] - \boldsymbol{w}_I||^2\right) \triangleq G_S^{\text{lb}}[m], \end{aligned} \tag{15}$$

where

$$\zeta_S^k[m] = \frac{\eta_S[m]}{\ln 2(\eta_S[m] + ||\boldsymbol{w}_U^k[m] - \boldsymbol{w}_I||^2 + (H_U - H_I)^2)(||\boldsymbol{w}_U^k[m] - \boldsymbol{w}_I||^2 + (H_U - H_I)^2)}. \tag{16}$$

In the same way, in the $k$th iteration, the lower-bound of $R_D[m]$, denoted as $G_D^{\mathrm{lb}}[m]$, can be obtained as

$$\begin{aligned} G_D[m] \geq \log_2 &\left(1+\frac{\eta_D[m]}{||\boldsymbol{w}_U^k[m]-\boldsymbol{w}_D||^2+H_U^2}\right) \\ &-\zeta_D^k[m]\left(||\boldsymbol{w}_U[m]-\boldsymbol{w}_D||^2-||\boldsymbol{w}_U^k[m]-\boldsymbol{w}_D||^2\right) \triangleq G_D^{\mathrm{lb}}[m], \end{aligned} \tag{17}$$

where

$$\zeta_D^k[m]=\frac{\eta_D[m]}{\ln 2(\eta_D[m]+||\boldsymbol{w}_U^k[m]-\boldsymbol{w}_D||^2+H_U^2)(||\boldsymbol{w}_U^k[m]-\boldsymbol{w}_D||^2+H_U^2)}. \tag{18}$$

$G_S^{\mathrm{lb}}[m]$ and $G_D^{\mathrm{lb}}[m]$ are concave w.r.t $\boldsymbol{W}$. Taking $G_S^{\mathrm{lb}}[m]$ and $G_D^{\mathrm{lb}}[m]$ into ($\mathbf{P}2$) and rewrite it into a convex problem as

$$(\mathbf{P}3): \max_{\boldsymbol{W}} \ \xi \tag{19a}$$

$$\text{s.t.} \ \ (1), \tag{19b}$$

$$\frac{1}{M}\sum_{m=1}^{M}\min\{G_S^{\mathrm{lb}}[m], G_D^{\mathrm{lb}}[m]\} \geq \xi, \tag{19c}$$

which can be solved easily.

### 3.3 Optimization of Transmit Power

By fixing the phase shifter of IRS $\boldsymbol{\Phi}$ and the UAV's trajectories $\boldsymbol{W}$, the UAV's transmit power $\boldsymbol{P}$ can be optimized in this section. For tractability, we define

$$\tau_S[m]=\frac{P_S\gamma^2N^2}{d_{SI}^2(||\boldsymbol{w}_U[m]-\boldsymbol{w}_I||^2+(H_U-H_I)^2)}, \tag{20}$$

$$\tau_D[m]=\frac{\gamma}{\sigma^2(||\boldsymbol{w}_U[m]-\boldsymbol{w}_D||^2+H_U^2)}. \tag{21}$$

Based on (20) and (21), we can respectively rewrite $R_S[m]$ and $R_D[m]$ as

$$L_S[m]=\log_2\left(1+\frac{\tau_S[m]}{\frac{P[m]}{\beta}+\sigma^2}\right), \tag{22}$$

$$L_D[m]=\log\left(1+\tau_D[m]P[m]\right). \tag{23}$$

Therefore, the subproblem of optimizing the transmit power at UAV can be expressed as

$$(\mathbf{P}4): \max_{\boldsymbol{P}} \ \xi \tag{24a}$$

$$\text{s.t.} \ \ (7), \tag{24b}$$

$$\frac{1}{M}\sum_{m=1}^{M}\min\{L_S[m], L_D[m]\} \geq \xi. \tag{24c}$$

$L_S[m]$ in constraints (24c) is convex w.r.t $\boldsymbol{P}$, which makes ($\mathbf{P}4$) hard to solve. Like the operation in the optimization of the UAV's trajectories, an approximate optimal solution can be obtained based on the successive convex optimization (SCA) method. We use the first-order Taylor expansion of $L_S[m]$ at $P^k[m]$ in the $k$th iteration. $L_S[m]$ can be given as

$$L_S[m] \geq \log_2\left(1+\frac{\tau_S[m]}{\frac{P^k[m]}{\beta}+\sigma^2}\right) - \mu_S^k[m]\left(P[m]-P^k[m]\right) \triangleq L_S^{\text{lb}}[m], \tag{25}$$

where

$$\mu_S^k[m] = \frac{\tau_S[m]/\beta}{\ln 2(\tau_S[m]+P^k[m]/\beta+\sigma^2)(P^k[m]/\beta+\sigma^2)}. \tag{26}$$

Therefore, ($\mathbf{P}4$) can be rewritten into a convex problem as

$$(\mathbf{P}5): \max_{\boldsymbol{P}} \ \xi \tag{27a}$$

$$\text{s.t.} \quad (7), \tag{27b}$$

$$\frac{1}{M}\sum_{m=1}^{M}\min\{L_S^{\text{lb}}[m], L_D[m]\} \geq \xi, \tag{27c}$$

### 3.4 Overall Algorithm

In summary, the optimal transmission rate $R^*$ is obtained by the value of the IRS phase shifter $\boldsymbol{\Phi}^*$, the UAV's trajectories $\boldsymbol{W}^*$ and the UAV's transmit power $\boldsymbol{P}^*$ by Algorithm 1.

## 4 Simulation Result

In this section, numerical results are provided to evaluate the performance of the proposed algorithm in the IRS-assisted FD UAV-based mobile relaying communication. The coordinates of $S$, $D$, $IRS$, $w_0$, $w_f$ are $[0, -200]$ m, $[-150, -50]$

**Algorithm 1.** Overall Algorithm

```
Input: $\boldsymbol{W}^{(0)}$, $\boldsymbol{P}^{(0)}$, $\boldsymbol{\Phi}^{(0)}$, $\epsilon$, $k = 0$
Output: $\boldsymbol{W}^*$, $\boldsymbol{P}^*$, $\boldsymbol{\Phi}^*$, $R^*$
do
    $k \leftarrow k + 1$
    obtain $\boldsymbol{W}^{(k)}$ with given $\boldsymbol{P}^{(k-1)}$ by ($\mathbf{P}3$)
    obtain $\boldsymbol{\Phi}^{(k)}$ with given $\boldsymbol{W}^{(k)}$ by (10)
    obtain $\boldsymbol{P}^{(k)}$ with given $\boldsymbol{W}^{(k)}$ by ($\mathbf{P}5$)
    obtain $R^{(k)}$ with given $\boldsymbol{W}^{(k)}$, $\boldsymbol{\Phi}^{(k)}$ and $\boldsymbol{P}^{(k)}$ by (6)
while $\frac{R^{(k)}-R^{(k-1)}}{R^{(k)}} > \epsilon$
$\boldsymbol{W}^* \leftarrow \boldsymbol{W}^k$
$\boldsymbol{\Phi}^* \leftarrow \boldsymbol{\Phi}^k$
$\boldsymbol{P}^* \leftarrow \boldsymbol{P}^k$
$R^* \leftarrow R^k$
```

m, $[0, -100]$ m, $[-200, 200]$ m, $[200, 200]$ m, respectively. The height of IRS and UAV are $H_I = 10$ m and $H_U = 30$ m. The remaining parameters inspired by [19] are summarized in Table 1.

**Table 1.** Simulation parameters

| Parameters | Example values |
|---|---|
| Maximum speed of the UAV, $V_{\max}$ | $20\,\text{m/s}$ |
| Time slot length, $\tau$ | $1\,\text{s}$ |
| Noise variance, $\sigma^2$ | $-110$ dBm |
| Reference channel gain at 1 m, $\gamma$ | $-20$ dB |
| Self-interference cancellation coefficient, $\beta$ | 100 dB |
| Antenna separation $d_0$ | $\lambda_0/2$ |
| Average transmission power of UAV, $\bar{P}$ | 0.1 W |
| Peak transmission power of UAV, $P_{\max}$ | 0.4 W |
| Transmission power of $S$, $P_S$ | 0.1 W |
| Tolerance, $\epsilon$ | $10^{-4}$ |

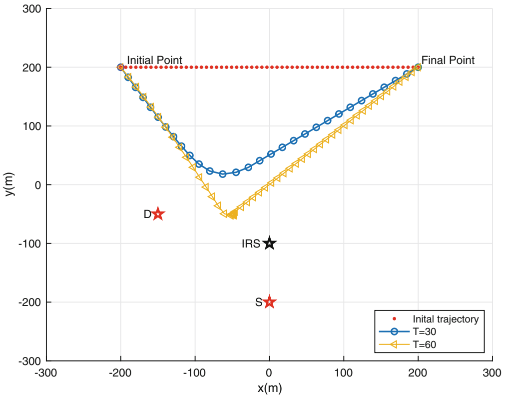

**Fig. 2.** Trajectories of the UAV with different $T$.

Figure 2 shows the trajectories of UAV in different flight time $T$ with $N = 256$. It is obvious that for different flight time, the UAV's trajectory is obviously different. When $T$ is equal to 60 s, the UAV first flies to the optimal position and hovers for a period of time before flying to the final point. In terms of $T = 30$ s, the UAV does not fly to a similar optimal position hovering due to the limitation of time. It flies as close to $D$ and IRS as possible and then flies to the final point. It is worth noting that the UAV tends to come close to the midpoint of $D$ and IRS because UAV can not communicate with $S$ directly in our scenario.

Figure 3 illustrates the average rates with different $N$ in the iteration. As the number of iterations increases, the average rates quickly stabilize at stable values. Furthermore, with the number of IRS elements $N$ increasing, the average rate increases significantly. With $N$ increasing from 64 to 256, almost 25% of the transmission rate increases. It shows that the assistance of the IRS not only establish a communication link between $S$ and UAV, but also can effectively improve the transmission performance of the system by appropriately increasing the number of IRS elements.

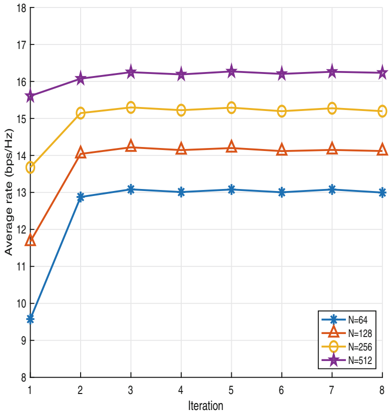

**Fig. 3.** Average rate with different $N$ of the IRS versus Iteration

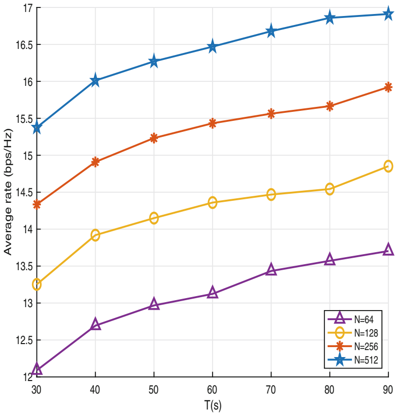

**Fig. 4.** Average rate with different $N$ of the IRS versus $T$

Figure 4 compares the average rate of the different $N$ under several values of flying time $T$. It is clear that as $T$ increasing, the average rates increase significantly. It is because the UAV has more time to hover around the optimal point of a greater $T$. Moreover, the influence of the number of elements $N$ also has a significant impact on system performance. It is straightforward that the average rate increases with the increase of $N$, which inspires us to use an IRS-assisted system to enhance the transmission performance of the communication system.

## 5 Conclusion

In this paper, we investigated an IRS-assisted DF UAV-based relay system. We jointly optimized the UAV's trajectory, the phase shifter of IRS, and transmit power of the UAV to maximize the average rate of the system. The non-convexity of the formulated problem results in solving the problem directly intractable. Therefore, we proposed an iterative algorithm on the basis of block coordinate descent and the SCA method. Numerical results show that the proposed scheme can significantly improve the transmission rate, which can solve the transmission problem in crowded cities in the future. Besides, the 3D trajectory design is left as the future work.

**Acknowledgments.** This work is supported in part by the Shanghai Aerospace Science and Technology (SAST) Innovation Fund under Grant SAST2019-092.

## References

1. Boccardi, F., Heath, R.W., Lozano, A., Marzetta, T.L., Popovski, P.: Five disruptive technology directions for 5G. IEEE Commun. Mag. **52**(2), 74–80 (2014). https://doi.org/10.1109/MCOM.2014.6736746
2. Wu, Q., Zhang, R.: Intelligent reflecting surface enhanced wireless network via joint active and passive beamforming. IEEE Trans. Wirel. Commun. **18**(11), 5394–5409 (2019). https://doi.org/10.1109/TWC.2019.2936025
3. Basar, E., Di Renzo, M., De Rosny, J., Debbah, M., Alouini, M., Zhang, R.: Wireless communications through reconfigurable intelligent surfaces. IEEE Access **7**, 116753–116773 (2019). https://doi.org/10.1109/ACCESS.2019.2935192
4. Gong, S., et al.: Toward smart wireless communications via intelligent reflecting surfaces: a contemporary survey. IEEE Commun. Surv. Tutor. **22**(4), 2283–2314 (2020). https://doi.org/10.1109/COMST.2020.3004197
5. Abeywickrama, S., Zhang, R., Wu, Q., Yuen, C.: Intelligent reflecting surface: practical phase shift model and beamforming optimization. IEEE Trans. Commun. **68**(9), 5849–5863 (2020). https://doi.org/10.1109/TCOMM.2020.3001125
6. Wu, Q., Zhang, S., Zheng, B., You, C., Zhang, R.: Intelligent reflecting surface aided wireless communications: a tutorial. IEEE Trans. Commun. **69**, 3313–3351 (2021). https://doi.org/10.1109/TCOMM.2021.3051897
7. Zuo, J., Liu, Y., Qin, Z., Al-Dhahir, N.: Resource allocation in intelligent reflecting surface assisted NOMA systems. IEEE Trans. Commun. **68**(11), 7170–7183 (2020). https://doi.org/10.1109/TCOMM.2020.3016742
8. Nadeem, Q.U.A., Kammoun, A., Chaaban, A., Debbah, M., Alouini, M.S.: Asymptotic max-min SINR analysis of reconfigurable intelligent surface assisted miso systems. IEEE Trans. Wirel. Commun. **19**(12), 7748–7764 (2020). https://doi.org/10.1109/TWC.2020.2986438
9. Yang, L., Yang, Y., Hasna, M.O., Alouini, M.S.: Coverage, probability of SNR gain, and DOR analysis of RIS-aided communication systems. IEEE Wirel. Commun. Lett. **9**(8), 1268–1272 (2020). https://doi.org/10.1109/LWC.2020.2987798
10. Gupta, L., Jain, R., Vaszkun, G.: Survey of important issues in UAV communication networks. IEEE Commun. Surv. Tutor. **18**(2), 1123–1152 (2016). https://doi.org/10.1109/COMST.2015.2495297
11. Zhang, C., Fu, W.: Optimal model for patrols of UAVs in power grid under time constraints. Int. J. Perform. Eng. **17**(1), 103 (2021)
12. Fotouhi, A., et al.: Survey on UAV cellular communications: practical aspects, standardization advancements, regulation, and security challenges. IEEE Commun. Surv. Tutor. **21**(4), 3417–3442 (2019). https://doi.org/10.1109/COMST.2019.2906228
13. Wu, L., Wang, W.: Resource allocation optimization of UAVs-enabled air-ground collaborative emergency network in disaster area. Int. J. Perform. Eng. **15**(8), 2133 (2019). https://doi.org/10.23940/ijpe.19.08.p13.21332144

14. Choi, D.H., Kim, S.H., Sung, D.K.: Energy-efficient maneuvering and communication of a single UAV-based relay. IEEE Trans. Aerosp. Electron. Syst. **50**(3), 2320–2327 (2014). https://doi.org/10.1109/TAES.2013.130074
15. Zhang, S., Zhang, H., He, Q., Bian, K., Song, L.: Joint trajectory and power optimization for UAV relay networks. IEEE Commun. Lett. **22**(1), 161–164 (2018). https://doi.org/10.1109/LCOMM.2017.2763135
16. Yang, L., Chen, J., Hasna, M.O., Yang, H.: Outage performance of UAV-assisted relaying systems with RF energy harvesting. IEEE Commun. Lett. **22**(12), 2471–2474 (2018). https://doi.org/10.1109/LCOMM.2018.2876869
17. Yang, L., Meng, F., Zhang, J., Hasna, M.O., Renzo, M.D.: On the performance of RIS-assisted dual-hop UAV communication systems. IEEE Trans. Veh. Technol. **69**(9), 10385–10390 (2020). https://doi.org/10.1109/TVT.2020.3004598
18. Zhang, S., Zhang, H., Di, B., Song, L.: Joint trajectory and power optimization for UAV sensing over cellular networks. IEEE Commun. Lett. **22**(11), 2382–2385 (2018). https://doi.org/10.1109/LCOMM.2018.2868075
19. Li, S., Duo, B., Yuan, X., Liang, Y., Di Renzo, M.: Reconfigurable intelligent surface assisted UAV communication: joint trajectory design and passive beamforming. IEEE Wirel. Commun. Lett. **9**(5), 716–720 (2020)